Optimizing Rail Temperature Management: A Time-Segmented K-Means Approach for Risk Mitigation and Resilient Infrastructure

Ferhat Çeçen[1*], Mehmet Saltan[2] and Ömer Faruk Acar[3]

[1] Süleyman Demirel University, Göller Bölgesi Teknokent Coordinatorship, Çünür, Süleyman Demirel Cd., 32260 Isparta, Türkiye, cecenferhat@sdu.edu.tr

[2] Süleyman Demirel University, Department of Civil Engineering, Çünür, Süleyman Demirel Cd., 32260 Isparta, Türkiye, mehmetsaltan@sdu.edu.tr

[3] Süleyman Demirel University, Department of International Trade and Logistics, Çünür, Süleyman Demirel Cd., 32260 Isparta, Türkiye, omeracar@sdu.edu.tr

* Corresponding author

Abstract: Proactive rail temperature management is vital for ensuring the structural integrity and safety of railway infrastructure, particularly to mitigate risks like thermal buckling and derailments. Existing empirical models, such as those by Hunt and Whittingham, have significant limitations in precision and adaptability, prompting the need for innovative approaches that align with modern infrastructure management practices. This study presents a novel methodology to optimize rail temperature prediction through time segmentation via K-means clustering. This approach represents a significant advancement in life cycle performance and risk assessment by providing a scalable, user-friendly solution. The proposed model integrates multivariate regression and Python-based automation to establish a relationship between air temperature, time, and rail temperature, designed for implementation in common spreadsheet tools like Microsoft Excel. Field validation across five Amtrak network stations, representing diverse climatic and structural conditions, demonstrated high predictive accuracy, with temperature deviations within ±2°C and an R^2 value of 0.943. This research contributes to resilient infrastructure management by enabling precise, low-cost temperature predictions, facilitating timely maintenance strategies, and enhancing risk-based decision making processes for railway operations.

Keywords: rail temperature; resilient infrastructure; risk management; life cycle analysis; k-means clustering

1 Introduction

Rail is recognized as one of the safest modes of transportation. However, like other modes of transport, unexpected heat waves and changing climatic conditions can have a significant negative impact on rail systems. These changes can affect the geometric stability of the tracks, potentially compromising safety [1]. Therefore, systematic track monitoring and proactive management of geometric deterioration have become essential strategies to mitigate emerging risks and ensure the continued safety and operational integrity of rail networks [2, 3]. Heat-related rail failure is one of the most significant threats to rail safety. Different countries use various terms to describe heat-related rail failure. For example, in the United States of America (USA), it is commonly known as "sun kink," in the United Kingdom (UK) as "rail buckling" [4]. In this study, this phenomenon is briefly referred to as RTB (rail thermal buckling). Some minor RTB incidents, such as those shown in Figure 1.a [5], may be difficult to detect through visual inspection alone. However, they can pose a safety risk, particularly at high speeds [6]. In addition, as shown in Figures 1.b-f [7-10], some S- or C-shaped RTBs can extend to large dimensions and cause derailments even when trains are running at speeds slightly above the restricted limits (e.g. 30 km/h).

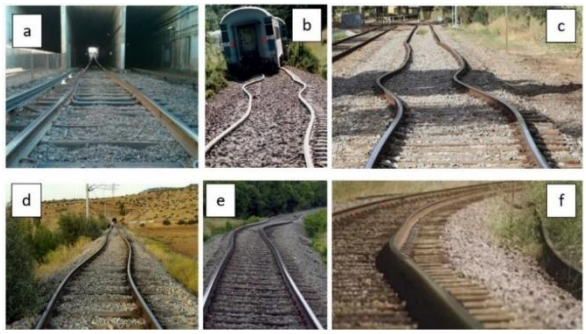

Figure 1
RTB samples from various countries; a) Washington, D.C., USA [5], b) Sweden [7], c) Unspecified line [8], d) Kahramanmaraş, Türkiye [9], e) Canada [7], f) Unspecified line [10]

As shown in Figure 1, RTB incidents have become a widespread global problem and are no longer confined to specific regions such as continental or desert climates [4, 6, 11, 12]. Climate change is a major factor contributing to the increasing frequency of RTB incidents, which have intensified in recent decades [11, 13]. Another factor contributing to the increasing trend of RTB incidents is the use of welded rail joints, which have been examined in detail in the literature [14]. While these joints offer significant advantages, they also extend the continuous rail length,

thereby increasing susceptibility to thermal expansion and contraction. In the USA, over 2,100 train derailments in the last forty years have been associated with track buckling, averaging approximately 50 accidents per year [15]. In the European Union (EU), Figure 2.a shows the recorded incidents due to lateral misalignment and annual temperature anomalies from 2008 to 2018 [6]. On the other hand, Ferranti et al. (2016) analysed more than 340,000 heat-related failures and incidents in the UK (South East England) from 2006 to 2013, the results of which are shown in Figure 2.b [12]. These analyses show a steady annual increase in RTB incidents, which correlates with global warming trends. Furthermore, as shown in Figure 2.b, some countries report RTB incidents almost all year round, not just in the summer, although the highest number of incidents occurs in July.

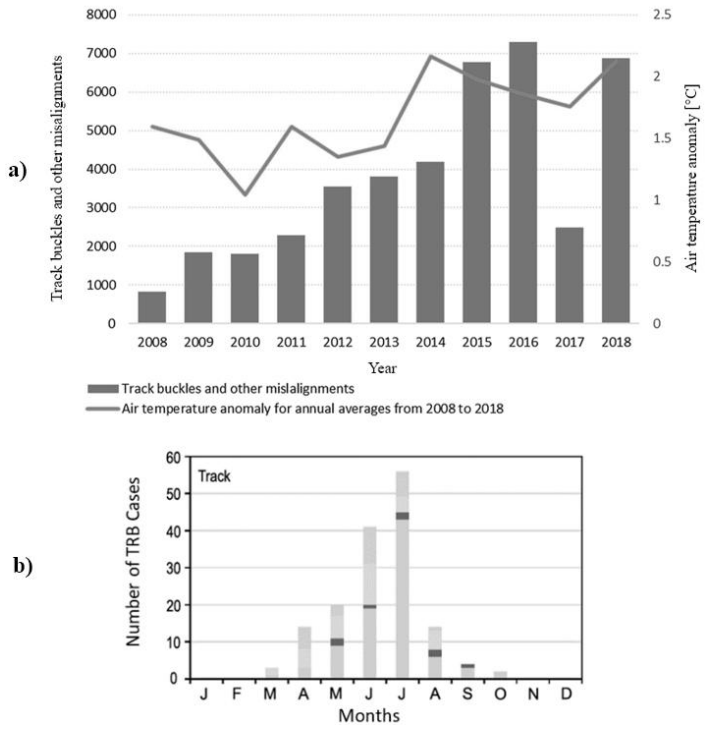

Figure 2

The relationship between the track misalignment and annual air temperature records in the EU [6], b) Monthly changes in the RTB incidents recorded in the UK [12]

In summary, this introduction has outlined the critical challenges posed by RTB incidents and highlighted the impact of changing climatic conditions and structural factors on rail safety. Building on this background, the following section reviews the literature on key benchmarks and temperature thresholds essential for the effective management of RTB. This discussion provides a foundation for understanding how quantitative approaches can be applied to mitigate RTB risks.

2 Benchmarks and Thresholds for RTB Management

To prevent RTB incidents, railway engineers use two key benchmarks: the Stress-Free Temperature (SFT) and the Critical Rail Temperature (CRT). The SFT, also known as the Rail Neutral Temperature (RNT), is a theoretical temperature at which the total stress in the rail, excluding residual stress, is zero. At this temperature, the rails in the track are the same length as they would be in an unstressed state. On the other hand, CRT values indicate the rail temperature above which RTB is likely to occur [6, 8, 16, 17]. These benchmarks (SFT and CRT) have been calculated from weather and rail temperature records using the equations given in Equations 1-12 [11, 18, 19].

$$T_{air_{avg}} = \frac{T_{air_{min}} + T_{air_{max}}}{2} \quad (1)$$

$$T_{rail_{min}} = T_{air_{min}} \quad (2)$$

$$T_{rail_{max-1}} = T_{air_{max}}\ x\ 1.5 \quad (3)$$

$$T_{rail_{max-2}} = T_{air_{max}} + 17℃ \quad (4)$$

$$T_{rail_{max-3}} = 1.228\ x\ T_{air_{max}} + \ 9.7℃ \quad (5)$$

$$T_{rail_{avg}} = \frac{T_{rail_{min}} + T_{rail_{max}}}{2} \quad (6)$$

$$SFT = T_{avg} + 5°C \quad (7)$$

$$T_{allw_{min}} = SFT - 3°C \quad (8)$$

$$T_{allw_{max}} = SFT + 3°C \quad (9)$$

$$CRT_{alarm} = \begin{cases} SFT + 10°C, & inadequate\ ballast\ support, etc. \\ SFT + 32°C, & good\ condition\ track \end{cases} \quad (10)$$

$$CRT_{50/100} = \begin{cases} SFT + 13°C, & inadequate\ ballast\ support, etc. \\ SFT + 37°C, & good\ condition\ track \end{cases} \quad (11)$$

$$CRT_{30} = \begin{cases} SFT + 15°C, & inadequate\ ballast\ support, etc. \\ SFT + 42°C, & good\ condition\ track \end{cases} \quad (12)$$

$Tair_{avg}$: Average annual air temperature, [°C]

$Tair_{min}$: Minimum recorded air temperature (e.g., over last 50 years), [°C]

$Tair_{max}$: Maximum recorded air temperature (e.g., over last 50 years), [°C]

$Trail_{min}$: Lowest possible rail temperature, [°C]

$Trail_{max\text{-}1}$: Highest possible rail temperature (Hunt Equation 1), [°C]

$Trail_{max\text{-}2}$: Highest possible rail temperature (Hunt Equation 2), [°C]

$Trail_{max\text{-}3}$: Highest possible rail temperature (Whittingham Equation), [°C]

$Trail_{avg}$: Average estimated rail temperature, [°C]

SFT : Stress-free temperature, [°C]

$Tallw_{min}$: Minimum allowed rail temperature, [°C]

$Tallw_{max}$: Maximum allowed rail temperature, [°C]

CRT_{alarm} : Alarm threshold for rail temperature, [°C]

$CRT_{50/100}$: Threshold for moderate speed restriction (e.g., 50–100 km/h), [°C]

CRT_{30} : Threshold for severe speed restriction (e.g., 30 km/h), [°C]

Railway engineers manage SFT to balance the stresses on the rails—compressive forces in summer and tensile forces in winter. By setting SFT midway between these extremes, they minimize these stresses [20]. Using historical weather data and Equations 1-12, engineers choose installation days with air temperatures close to the SFT or pre-stress the rails to match the SFT [11, 18]. In this context, Equation 1 calculates the average air temperature ($Tair_{avg}$) by averaging the annual minimum ($Tair_{min}$) and the annual maximum ($Tair_{max}$) temperatures obtained from the long-term temperature database (e.g., the last 50 years) for the relevant railroad section. Equation 2 is used to estimate the lowest possible rail temperature ($Trail_{min}$), whereas Equations 3 and 4 are used to estimate the highest possible rail temperature ($Trail_{max\text{-}1}$ and $Trail_{max\text{-}2}$). These equations were proposed by Hunt (1994) [21, 22]. Notably, the second equation yields higher rail temperature values at lower air temperatures. Although not as widely used as the equations proposed by Hunt (1994), an earlier equation by Whittingham (1969), presented as Equation 5, is also referenced in the literature [19]. Additionally, Esveld proposed a graphical method to estimate rail temperatures under sunny and cloudy conditions [16]. Equation 6 defines the average rail temperature (*Trailavg*) as the arithmetic mean of *Trailmin* and one of the maximum values ($Trail_{max}$) obtained from the Hunt or Whittingham equations. The SFT value is then calculated as 5°C higher than this $Trail_{avg}$ value (Eq. 7). If the ambient temperature during installation differs significantly from the SFT, the rails are pre-stressed to the SFT length using special equipment. SFT values vary from country to country and in some cases from city to city within countries. According to the literature [16, 18], SFT values are 25°C in France and Switzerland, 27°C in the UK and Spain, 17-22°C in Germany, 13-36°C in Türkiye and 35-43°C in the USA.

Once these SFT values have been determined, engineers calculate the temperature limits within which maintenance or installation work can be safely carried out. Equations 8 and 9 are among the most commonly used equations for this purpose. These equations calculate the minimum ($Tallw_{min}$) and maximum ($Tallw_{max}$) allowed rail temperatures for maintenance/installation at the railway section, respectively. After determining SFT values, CRT values are calculated using safety coefficients based on track conditions, such as ballast support. These coefficients vary depending on the railway organization, infrastructure, and operating speed. Equations 10-12 give values from the literature [11]. When rail temperature readings exceed the alarm threshold (CRT_{alarm}) , inspections are intensified and track conditions are thoroughly assessed by experts. If temperatures exceed a second threshold ($CRT_{50/100}$), emergency speed restrictions (between 50 and 100 km/h, depending on train and track type) are implemented. When temperatures exceed the third threshold (CRT_{30}), severe speed restrictions (30 km/h) are imposed and non-essential services are cancelled. Speed restrictions are necessary because RTB incidents usually occur when a train is passing, as rails rarely buckle spontaneously even at high temperatures and usually require additional energy input from passing trains [11, 12]. Although these restrictions cause delays, they are essential to ensure safety and protect life and property [23]. Different definitions/applications of each country/railway operator are also possible. According to the active monitoring system of Amtrak (USA), the rail temperature set points are 51.7°C for warning, 52.8°C for alarm, and 57.2°C for critical alarm. In addition to rail temperatures, air temperatures are also monitored to ensure safe transport. The air temperature set points are 33.9°C for warning, 35.0°C for alarm, and 38.9°C for critical alarm, according to the same monitoring system [24]. This is because the temperature sensors that are connected to the rails both take local measurements and can easily be subject to error or failure. Using Equations 1-12 to determine SFT and CRT values can be misleading. Recent studies, like the case in Figure 3, show the conventional equations by Hunt and Esveld may not accurately predict rail temperatures. For instance, at 23°C air temperature, rail temperatures can range from 21°C to 43°C. Equations such as Esveld's (sunny conditions) and Hunt's (Eq. 4) give high rail temperature predictions (40-42°C), leading to unnecessary precautions and economic losses. Conversely, moderate equations may underestimate temperatures, increasing the risk of rail track buckling (RTB) and accidents. Therefore, it can be concluded that conventional approaches are insufficient for effectively preventing RTB incidents.

Engineers and researchers, recognizing the limitations of conventional equations, have developed two new approaches. The first approach uses more complex relationships involving variables like wind speed, rail orientation, pressure, humidity, and solar radiation, rather than just air temperature. Equation 13, found in the literature, contains 28 coefficients and variables. A study compared actual rail temperatures in July (9-14 June 2010) with those calculated using Equation 13 (T_{rail}) and the methods by Hunt and Whittingham.

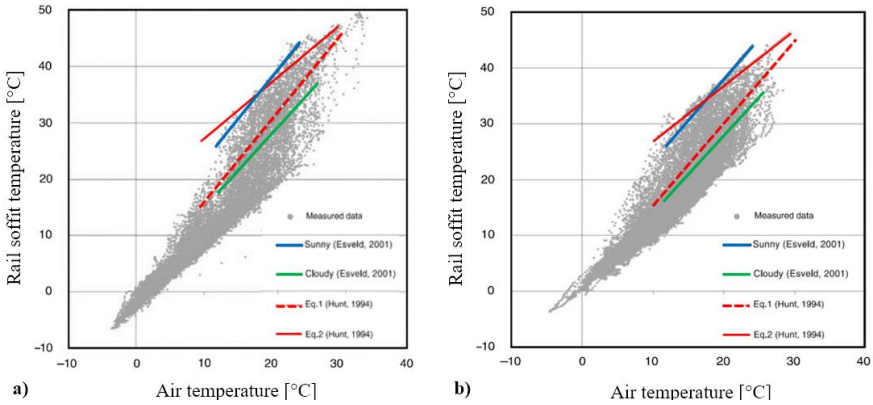

Figure 3

Air versus rail temperature records for two different railway sections in the UK including the numerical empirical equations given the other researchers [16]

While the complex equation provided better predictions, it still had a 6°C difference [19]. Since the detailed descriptions of the 28 symbols used in that equation are already provided in the referenced study [19], they are not repeated here to maintain clarity and avoid redundancy.

$$T_{rail} = \beta_{1_{\mu 10}} + \beta_{2_{\mu 10}} + \beta_{3_{temp\_scrn}} + \beta_{4_{dewpt\_scrn}} + \beta_{5_{sfc\_pres}} + \beta_{6_{accum\_prcp}} + \beta_{7_{mslp}} + \beta_{8_{accum\_evap}} + \beta_{9_{lat\_liflx}} + \beta_{10_{hfsfcdown}} + \beta_{11_{av\_nethsfc}} + \beta_{12_{av\_netswsfc}} + \beta_{13_{av\_olr}} + \beta_{14_{av\_sens\_lflx}} + \beta_{15_{av\_sfc\_sw\_dif}} + \beta_{16_{av\_sfc\_sw\_dir}} + \beta_{17_{av\_swirrtop}} + \beta_{18_{av\_swfcdwn}} + \beta_{19_{mid\_cld}} + \beta_{20_{gsair\_scrn}} + \beta_{21_{sens\_lflx}} + \beta_{22_{sfc\_temp}} + \beta_{23_{soil\_mois}} + \beta_{24_{soil\_temp}} + \beta_{25_{\max\_scrn}} + \beta_{26_{\min\_scrn}} + \beta_{27_{tll\_cld}} + \beta_{28_{Z0}} \quad (13)$$

The second approach is to take advantage of rail temperature monitoring systems. Due to the difficulty in obtaining the necessary data for complex equations, such as Equation 13, and concerns about the reliability of each input, some researchers/organizations have evaluated that such applications are not feasible [25]. Therefore, several railway organizations have opted to measure rail temperature directly using sensors attached to the rails. While this approach provides a more reliable solution in theory, effective management of RTB cases requires a sensor network covering the entire rail network. This is because, as can be inferred from Figure 3, rail temperatures vary considerably from place to place, and using just a few sensors over a long distance would be insufficient. Therefore, some railway operators have started to extend these systems by installing numerous sensors on their tracks. Although this application involves significant costs for sensor installation, operation and maintenance, the importance of the issue and the need to make necessary decisions in critical areas forces them to make this effort. However, as pilot systems have been tested in the field, some important drawbacks have emerged. For example, there are safety concerns, especially on high-speed and

electrified lines. Because, the power sources (batteries) of these modular systems need to be replaced periodically. In addition, the sensors need to be constantly checked to ensure that they are calibrated and working correctly under different operating loads and climatic conditions. In addition, it is not always easy to transmit data wirelessly via the Internet or satellite along the route of the railway lines. While it is possible to address these issues, each solution comes with its own costs, deployment challenges and time and labour requirements.

Therefore, to prevent RTB incidents and to accurately predict, measure and analyze rail temperatures, the industry needs a less complex but more accurate/convergent, easy to use and freely available quantitative relationship. Although some railway organizations measure rail temperatures using sensors attached to the rails, it can be beneficial to compare sensor-induced data with numerical predictions. This approach helps to continuously monitor and easily address potentially faulty sensors. By using one or two input data from meteorological (weather) stations, which already exist in almost every town/station, the number of rail temperature sensors that need to be installed on railways can be significantly reduced or in some cases eliminated. This would also overcome the disadvantage of not having historical rail temperature data to determine SFT and CRT. In addition, the use of future meteorological forecasts can make rail operations more efficient.

2 Method

In this study, a specific Python script was used to achieve the objectives outlined in the previous section. This script uses common spreadsheet files (e.g. xlsx files) as a database. To generate the required relationships, the spreadsheet files must contain at least three columns: time (in clock format, i.e. hh:mm), air temperature and actual rail temperature. The script parses the time data into hours and minutes. It then uses the air temperature, hour and minute as the "independent" variables, while the rail temperature is used as the "dependent" variable. Using the K-means clustering algorithm, a common method in machine learning, the script is able to divide the 24-hour data into a preferred number of segments (time intervals). In this study, it was decided to segment the dataset into three parts (K = 3 clusters). The script determines the optimal start and end times for each segment using the K-means clustering algorithm [26]. After these, a multivariate regression model is trained for each time segment. The trained models are then used to predict rail temperatures. As a result, three different equations (functions) that best match the actual rail temperature values (with high R^2 values) are determined for the three different time segments of the day. These equations are combined into a single output that can be used in common spreadsheet software such as Microsoft Office Excel using IF/AND functions. While the method of predicting rail temperatures using machine learning algorithms has been the subject of several studies in recent years [25, 27], the novel aspect of this study is the analysis of measurement days by dividing them

into three segments via K-means clustering method and finally presenting the results in an easy-to-use and free-for-access numerical formula. Moreover, the formula requires very little data (only air temperature and time of day variables) and is simple enough to run on a simple spreadsheet or by hand if desired. This makes it easy to obtain real-time, predicted or historical rail temperature values through simple calculations using the almost ubiquitous time-indexed air temperature sensor networks or hourly weather forecasts/records provided by meteorological services.

The newly written Python script uses; 1) the actual rail temperature, 2) time (hour & minute; hh:mm), 3) air temperature variables, to generate the resulting numerical formula. Once this formula has been generated, no actual rail temperature values are required to calculate real-time, predicted or historical rail temperatures. In this case study, these three input data sets to generate the formula were obtained from the Amtrak's website. This website was developed as part of a Rail Temperature Prediction System (RTPS) project carried out in the USA. This project was one of the first in this field. This RTPS has been developed by ENSCO within a program supported by the Federal Railroad Administration (FRA) to provide more reliable decisionmaking when issuing slow orders to manage track buckling risk. The model is based on a transient heat transfer process and uses air temperature, solar radiation intensity, solar angle, wind speed, sky temperature, and the heat absorptivity and emissivity of the rail. Continuous efforts have been made to improve the model algorithm. Several valuable experiences have been gained, some of which have been shared with the public scientific community [23, 28, 29]. This RTPS was first tested on Amtrak's NEC in 2007. Amtrak, officially known as the National Railroad Passenger Corporation, provides open access to real-time rail temperature and meteorological data through its dedicated website [24]. The data streaming frequency (rail or air temperature) is 15-minute intervals and details of the most recent data (last 24 hours) can be accessed through this website.

In this study, the actual rail temperature (the first input variable mentioned above) was used to run Phyton scripts (machine learning algorithms) and validate the rail temperature predictions. The Amtrak wayside locations have four temperature sensors (left and right rails of parallel lines), so there are four different rail temperature variables (track 3 S, 3 N, 2 S, 2 N). The raw data from each sensor (rail temperature) is considered noisy by the developers [28], so filtering was applied to smooth the data. In addition, as discussed by them, significant differences were observed between these four sensors, so an average channel was created for the RTPS model [23, 28]. This average channel is not included on the Amtrak website [24]. In this study, the average of the two lowest sensors was used for analysis. This is because, depending on the position of the sun, for example, the western sides of the rails are shaded first during the morning and the eastern sides of the rails are shaded after midday. As a result, the shaded sides are well represented by the air temperature and the entire rail web. Therefore, the average of the two sensors with the lowest values (which change dynamically according to the position of the sun)

is used in this study. In this study, the outside air temperature data (the other input variable mentioned above) was also used to run the Phyton script and predict the rail temperatures. This data, along with the other variables (e.g. solar radiation, wind direction, wind speed, rain, atmospheric pressure), is streamed from the weather stations set up for the RTPS system. Some examples of these stations are shown in Figure 4 [28].

Figure 4
Several wayside weather stations (highlighted with red circles) along Amtrak's railroad lines [28]

This study analyzed data from five RTPS monitoring sites: BWI, Prince, Wilmington, Albany, and Monmouth stations. GPS coordinates were obtained from the Amtrak's website [24] and mapped using Google Earth [30], as presented as an example in Figure 5. Each site has unique railroad and climatic conditions:

- **BWI:** This station is part of Amtrak's Northeast Corridor, one of the busiest rail lines in the country, and frequently experiences speed restrictions due to extreme heat [31]. RTPS monitoring equipment is installed on three parallel tracks, with four sensors deployed. Coordinates: 39.19301°N, -76.69493°W. The site is surrounded by forest, with no structures providing shade. Similarly, SNCF (French National Railways) installs weather stations in shaded locations, typically on catenary masts [32].
- **Prince:** Near the ocean, partly surrounded by forest, with two parallel tracks and four sensors. Coordinates: 39.56908°N, -76.03831°W. High humidity levels were recorded, approaching 100% on some days.
- **Wilmington:** Three tracks (two concrete, one wooden sleepers) with four sensors installed. Coordinates: 39.74914°N, -75.51888°W. Located between a river and a residential area.
- **Albany:** On the Amtrak Empire Line, featuring four to five mixed-sleeper tracks with four sensors. Coordinates: 42.64388°N, -73.74093°W. Proximity to a platform roof may cause artificial shading and wind blocking.
- **Monmouth:** Rural area with four parallel tracks. Coordinates: 40.37651°N, -74.54739°W. No tall structures nearby to block wind or create shade.

Figure 5
Google Earth views of where BWI Station RTPS sensors are located [30]

As mentioned above, the RTPS data stream frequency is 15 minutes. Therefore, data was collected for 20 air temperatures, 20 rail temperatures and 20 time points every hour, giving a total of 1,440 data points per day (24 hours). Over a nine-day recording period, this resulted in 12,960 input data points being recorded in a spreadsheet. After running the script described, this data was found to be sufficient to determine the optimal start and end times for three segments of the day and to develop three numerical equations for each segment. Notably, all the data was collected in July 2024. This month was chosen because, according to various literature sources, it has the highest number of track buckling incidents in the northern hemisphere [12, 25]. In addition, weather records from meteorological institutions show that the analysed sites experienced almost all types of climatic conditions during this period, including sunny, cloudy, rainy, dry, windy and calm. While the equation developed is primarily applicable during the summer months and within certain states in the USA, similar procedures can be applied to other states or countries and time periods. By recording the data in a spreadsheet and analyzing it with the Python script described, it will be possible to determine the optimal start and end times for each segment and to identify the equations with the most overlap for each segment. On the other hand, if a single equation can be developed to represent these diverse and feature-rich sites, it could potentially be a significant achievement and applicable to many other rail lines, both within the USA and internationally.

3 Results

Figure 6 shows the variations of 4,320 actual rail temperature measurements over the course of the day, with different colors representing each station. As observed, most of the station data follows a recognizable pattern, with temperature values rising and falling systematically. However, the Albany station, in particular,

exhibits anomalies on some days that cannot be easily explained. This discrepancy will be analyzed in detail in the Discussion section.

Another notable aspect is the division of the day into three time segments (night, day to afternoon, and afternoon to midnight). It is evident that almost all stations display a similar trend of stability, increase, or decrease across these segments. The start and end times for the time segments were determined using the Python script described above to obtain optimal results. As seen in Figure 6: from 00:00 to about 08:00, the rail and air temperatures remain close together and approximately constant; from 08:00 to 16:00, solar radiation increases as the sun rises, causing both air and rail temperatures to rise rapidly and stabilize at a maximum level; and from 16:00 to 24:00, both air and rail temperatures exhibit a steady downward trend. These observations highlight the different temperature trends during the different segments of the day. After performing time segmentation using the K-means clustering algorithm in the Python script, a multivariate regression model was trained for each time segment using the 12,960 input data points recorded in a spreadsheet. As a result, three different equations were determined to best fit the actual rail temperature values for the three different time segments of the day. These equations are combined into a single output formula that can be used in common spreadsheet software such as Microsoft Office Excel using IF/AND functions. The combined formula is shown below as Equation 14. The R^2 value of this formula has been calculated by Phyton to be 0.943.

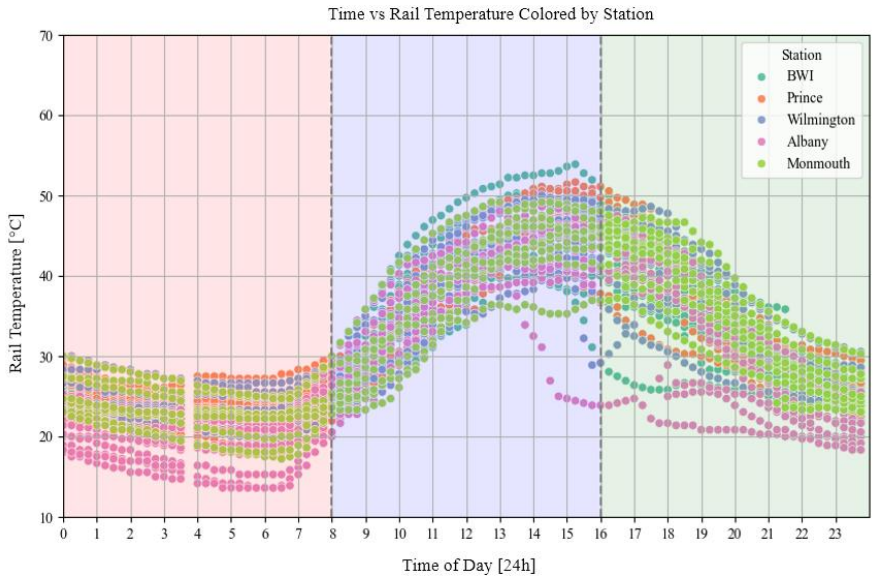

Figure 6

Rail temperature data on a station-by-station basis and over a 24-hour time period

$$Rail\_temp = \begin{cases} 1.0485 \times Air_{Temp} + 0.0870 \times Hour - 0.0011 \times Minute - 1.7509, \\ 00{:}00 \leq Time < 08{:}00 \\ 1.2935 \times Air_{Temp} + 0.8544 \times Hour + 0.0143 \times Minute - 9.9604, \\ 08{:}00 \leq Time < 16{:}00 \\ 1.2353 \times Air_{Temp} - 1.2080 \times Hour - 0.0159 \times Minute - 21.3464, \\ 16{:}00 \leq Time < 24{:}00 \end{cases} \quad (14)$$

Air_temp : Measured/recorded atmospheric air temperature at given times, [°C]

Rail_temp : Estimated rail temperature derived from Air_temp at corresponding time points, [°C]

Hour : The hour component of the time variable expressed on a 24-hour clock (0–23)

Minute : The minute component of the time variable (0–59)

Time : Daily time represented in HH:MM (24-hour) format, used to segment the day into three distinct periods

Figure 7 for BWI station shows the performance of the prediction equation for one of the five analysis sites. The air temperature (blue line), actual rail temperature (black line) from the Amtrak website [24], and the predicted rail temperature (green line) from Equation 14 were evaluated over the 9-day recording period. As seen, the actual and predicted rail temperature values overlap to a large extent on all days, including 16-17 July 2024, when the air temperature was around 40 °C, or 18-19 July 2024, when the air temperature was relatively low (29 °C), with a maximum difference of 2-3 °C, and the time with the peak temperature also overlaps to a large extent. These findings also apply to the Prince, Willington, and Monmouth stations.

4 Discussion

In this study, instead of using detailed data and sensors, a novel application was preferred that assumes; 1) there is no solar input at night, 2) solar radiation and temperature increase from sunrise to mid-afternoon, 3) solar radiation and radiant heat decrease from mid-afternoon to midnight, resulting in a gradual cooling of the atmosphere and Earth. This "three-segment air temperature-based rail temperature regulation" approach is the first known application in the literature that allows simple and practical thermal modelling without the need for additional sensors or detailed data. For a better interpretation, the differences between the results obtained from the Hunt, Whittingham and this study models compared to the actual rail temperature values are calculated in Celsius and presented on an hourly basis in Figure 8.

As can be seen, the newly developed relationship shows that the largest differences occur during the transitions between time segments, but do not exceed 2-3°C. This value is close to the error of the recently developed complex RTPS or the other similar systems [19, 23, 27-29]. Moreover, considering that the air temperature represents a broad location and that such variations would be expected if rail temperatures were measured across this broad geography, the 2-3°C difference might not even be considered a significant error. In fact, Figure 9 shows differences of up to 9°C between four closely spaced rail temperature sensors. On the other hand, conventional methods show differences of at least 5°C during peak temperatures around 15:00-16:00, with these differences increasing significantly at other times, approaching 20°C. Another issue is that a significant proportion of the differences seen in Figure 8 are from the Albany station data. This is likely to be due to the placement of the temperature sensors close to the platform roof and/or the rapid cooling of the rails due to rainfall, while the air temperature cools more slowly compared to the rails. The methodology used in this study suggests that the effect of the first possibility is significantly reduced. This is because, except for the days 16-18 July 2024 (7 out of the 9 days of the measurement period), there is a significant overlap. This success is remarkable even considering the large differences between the four sensors shown in Figure 9.

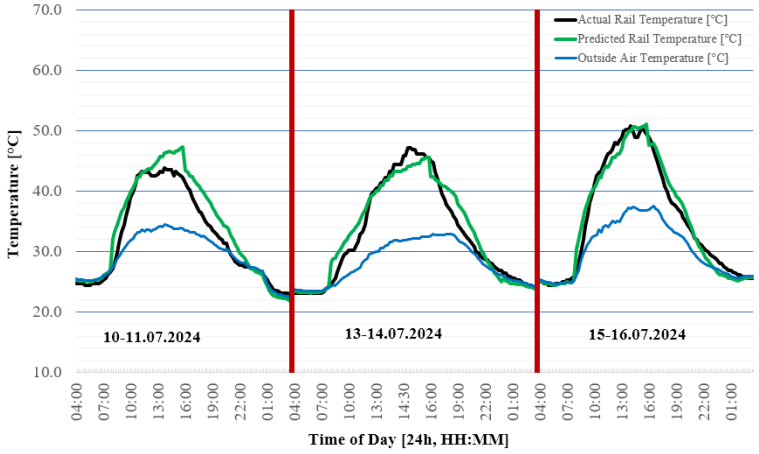

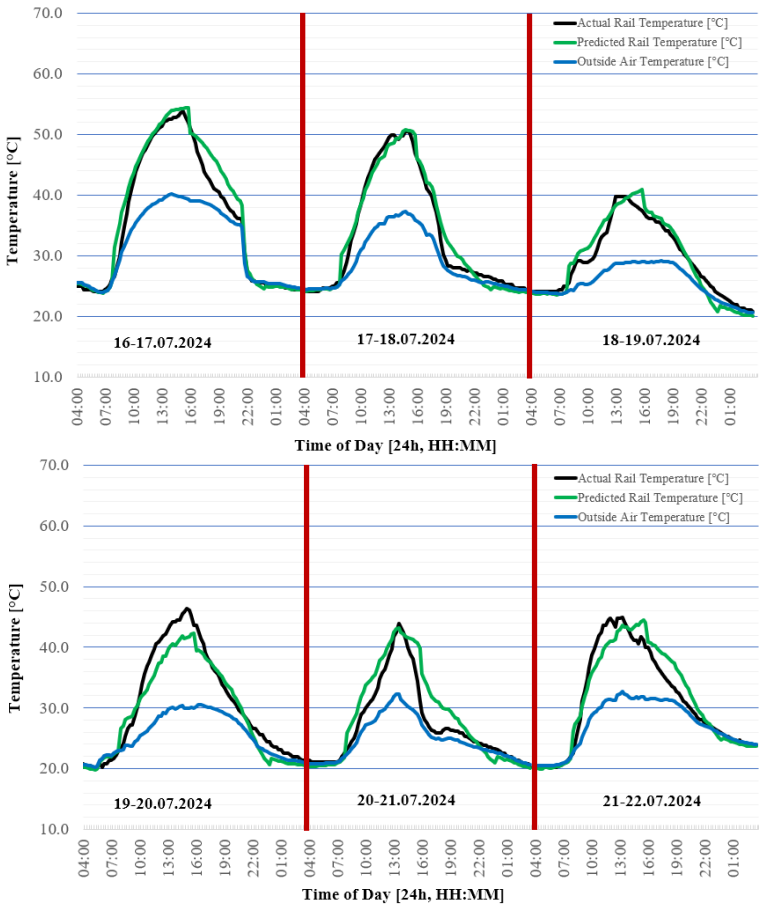

Figure 7
BWI Station rail temperature (actual and predicted) vs air temperature [°C] graphs

However, although there is an overlap in the peak temperature values on 16 and 18 July 2024, the actual rail temperature dropped rapidly due to the subsequent rainfall (as can be seen in Figure 10), while the air temperature did not drop as quickly, leading to an increased difference as the predicted rail temperature decreased more slowly. This suggests that the newly developed model may be weak in capturing sudden increases and decreases in rail temperature due to the slower response of air temperature. However, this disadvantage is also seen in most of the complex models developed to date. The RTPS developers found that the ambient temperature at ground level is typically 0.5-1°C higher than the ambient temperature measured 9 metres above ground [29]. Therefore, by adjusting the location of the weather station, a faster response can be achieved in some cases. On the other hand, as experienced by the ENSCO developers, the difference between the ambient temperature and the sky temperature can lead to overestimation or underestimation

of the peak rail temperature on certain days [29]. As seen, even the most advanced models developed today are not free from errors, and approximately 2.8°C peak value difference is considered normal even on ideal days [29]. Under these conditions, it seems that the new numerical method, which uses very little data and has been developed with pioneering approaches, is significantly more successful than conventional methods and often provides results comparable to modern complex models. However, expanding the research is undoubtedly necessary.

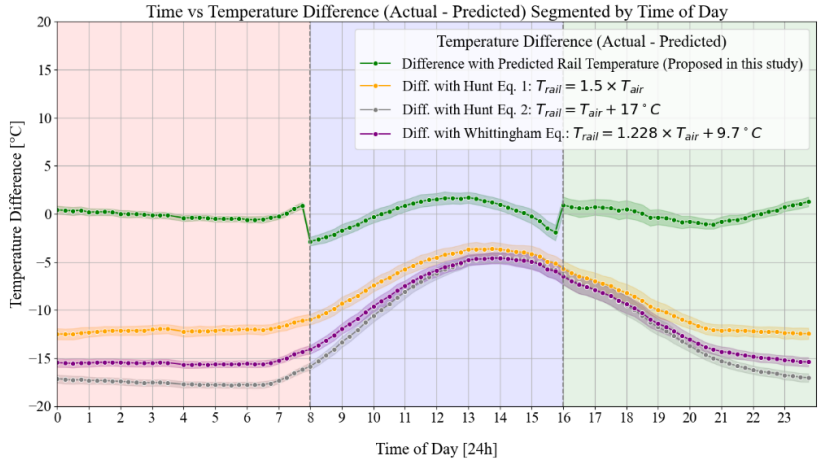

Figure 8

Difference between actual rail temperature and predictions by Hunt, Whittingham, and this study

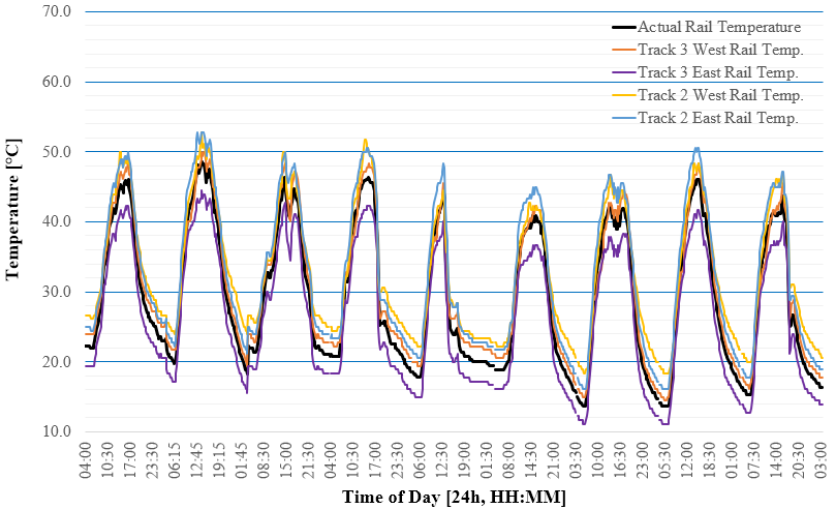

Figure 9

Temperature records from four rail temperature sensors in the vicinity of Albany station and the differences between each of them and the average

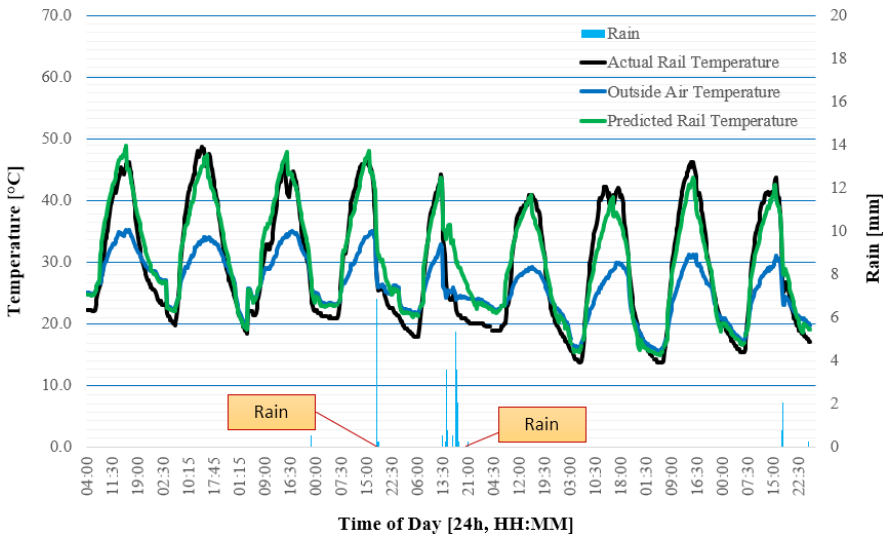

Figure 10
The sudden drop in rail temperature due to rain, in contrast to the relatively slow decrease in air temperature and the new air temperature-indexed equation (Albany Station)

Conclusions

Railway safety is increasingly affected by global warming and climate change, requiring robust and cost-effective strategies for monitoring and predicting rail temperatures. Traditional empirical equations, such as those proposed by Hunt and Whittingham, often lack precision, leading to either over-cautious measures or increased risk of rail thermal buckling (RTB). Conversely, while modern, multi-variable models and in-situ rail temperature measurements provide higher accuracy, they are resource-intensive and challenging to maintain over a system's life cycle.

This study introduces a novel, practical approach for rail temperature prediction, emphasizing simplicity, adaptability, and accuracy. The proposed method aligns with infrastructure management priorities by integrating minimal data requirements – air temperature and time of day – into a user-friendly prediction model suitable for widespread use. The findings of the study are summarized as follows:

- This study is the first in the literature to employ time-segmented modeling, leveraging the natural diurnal cycle of solar radiation and temperature changes. By dividing the day into night, day, and evening periods, the proposed model effectively eliminates the need for additional sensors. This innovative segmentation provides a practical and efficient solution that contributes to optimising life cycle performance and infrastructure resilience.

- The study leverages 12,960 data points to apply K-means clustering to determine the optimal time segmentation, and then trains regression models tailored to each segment. The resulting equations are integrated into a unified formula that can be executed in Microsoft Excel, delivering highly accurate predictions with an R^2 value of 0.943. This approach supports effective risk-based decision making by providing accessible and reliable temperature forecasts.
- The model exhibits accuracy comparable to complex Rail Temperature Predicting Systems (RTPS), with deviations maintained within ±2-3°C across transitions between time segments. This level of precision significantly outperforms conventional methods, which often show errors exceeding 5°C, particularly during peak temperature periods.
- The model is less effective at capturing sudden temperature changes caused by events such as rain, a limitation also shared by many advanced models. However, improving the placement of weather stations can enhance the model's responsiveness. Field validation conducted across a range of climatic conditions has demonstrated the robustness of this approach.
- Although this methodology was initially developed for summer conditions in certain regions of the USA, it can be adapted for use in different geographic and temporal settings. By recording and analyzing data using the provided Python script, users have the flexibility to adjust segment timings and tailor equations to suit the needs of local infrastructure.
- While the diurnal thermal patterns examined in this study reflect typical conditions of temperate climate zones, the underlying methodology – particularly the data-driven time segmentation – remains adaptable to nonstandard climatic regimes. This flexibility arises from the model's reliance on observable temperature trends rather than fixed assumptions. Furthermore, the approach could be further generalized through geographic segmentation, where an additional variable – based on climatic or latitudinal clustering – guides the selection of region-specific equations within spreadsheet-based applications. Such extensions, supported by local data collection or existing climate records, would maintain the model's operational simplicity while enhancing its applicability across broader rail networks.

In conclusion, the proposed model strikes a balance between simplicity and accuracy, providing a practical, cost-effective alternative to both traditional and modern approaches. Its potential to optimize rail temperature management and support proactive maintenance strategies suggests promising applications. However, limitations of the model in capturing abrupt temperature changes highlight the need for further research to improve its adaptability and accuracy under varying conditions. Improving the placement and density of nearby weather stations is expected to improve the model's accuracy and responsiveness without

compromising its simplicity or field applicability. Therefore, future studies should focus on refining this approach to address these limitations and improve its effectiveness across different scenarios.

Acknowledgement

This study used the actual rail and air temperature data published on Amtrak's open access website as part of the Rail Temperature Prediction System (RTPS), developed by ENSCO with support from the US Federal Railroad Administration (FRA) and initially deployed on Amtrak routes. The authors would like to thank these organizations and officials for their support in advancing public science and the development of new rail temperature prediction models

References

[1] Y. Luo, A Model for Predicting the Effect of Temperature Force of Continuous Welded Rail Track, Journal of Rail and Rapid Transit, Vol. 213, No. 1, 1999, pp. 117-124, https://doi.org/10.1243/0954409991531074

[2] D. Németh, H. Horváth, M. R. Movahedi, A. Németh, S. Fischer, Investigation of the Track Gauge in Straight Sections, Considering Hungarian Railway Lines, Acta Polytechnica Hungarica, Vol. 19, No. 3, 2022, https://acta.uni-obuda.hu/Nemeth_Horvath_Movahedi_Nemeth_Fischer_121.pdf

[3] Jóvér, L. Gáspár, S. Fischer, Investigation of Tramway Line No. 1, in Budapest, Based on Dynamic Measurements. Acta Polytechnica Hungarica, Vol. 19, No. 3, 2022, https://acta.uni-obuda.hu/Jover_Gaspar_Fischer_121.pdf

[4] F. Çeçen, B. Aktaş, Use of Thermal Imaging Cameras to Identify Best Locations for Rail Temperature Monitoring Systems (RTMS): Development of Rapid Analysis Methods, Railway Engineering, Vol. 20, No. 2, 2023, pp. 141-154, https://doi.org/10.47072/demiryolu.1474099

[5] PBS News, Heat Wave Causes Kinks in Rail Tracks, PBS News, July 7, 2010, Accessed July 30, 2024, https://www.pbs.org/newshour/world/heat-wave-causes-kinks-in-rail-tracks

[6] I. V. Sanchis, R. I. Franco, P. M. Fernández, P. S. Zuriaga, J. B. F. Torres, Risk of Increasing Temperature Due to Climate Change on High-speed Rail Network in Spain, Transportation Research Part D: Transport and Environment, Vol. 82, 2020, https://doi.org/10.1016/j.trd.2020.102312

[7] K. Dobney, Quantifying the Effects of an Increasingly Warmer Climate with a View to Improving the Resilience of the GB Railway Network: Is a New Stressing Regime the Answer? PhD Thesis, University of Birmingham, Department of Engineering, School of Civil Engineering, 2010, 191 p.

[8] E. Y. Chao, Development of a First-Generation Prototype Laboratory System for Rail Neutral Temperature Measurements, Master's Thesis, University of

South Carolina, College of Engineering and Computing, Civil Engineering Faculty, 2022, 63 p.

[9] Sıcaktan tren rayları bile genleşti! CNNTurk.com, August 3, 2010, Accessed July 30, 2024, https://www.cnnturk.com/turkiye/sicaktan-tren-raylari-bile-genlesti-11-12-2018

[10] G. Wolf, Preventing Track Buckles, Interface, March 10, 2005, Accessed July 30, 2024, https://interfacejournal.com/archives/644

[11] K. Dobney, C. J. Baker, L. Chapman, A. D. Quinn, The Future Cost to the United Kingdom's Railway Network of Heat-related Delays and Buckles Caused by the Predicted Increase in High Summer Temperatures owing to Climate Change, Journal of Rail and Rapid Transit, Vol. 224, No. 1, 2009, pp. 25-34, https://doi.org/10.1243/09544097JRRT292

[12] E. Ferranti, L. Chapman, C. Lowe, S. McCulloch, D. Jaroszweski, A. Quinn, Heat-related Failures on Southeast England's Railway Network: Insights and Implications for Heat Risk Management, Weather, Climate, and Society, Vol. 8, No. 2, 2016, pp. 177-191, https://doi.org/10.1175/WCAS-D-15-0068.1

[13] C. Ngamkhanong, C. M. Wey, S. Kaewunruen, Buckling Analysis of Interspersed Railway Tracks, Applied Sciences, Vol. 10, No. 9, 2020, https://doi.org/10.3390/app10093091

[14] S. Fischer, D. Harangozó, D. Németh, B. Kocsis, M. Sysyn, D. Kurhan, A. Brautigam, Investigation of Heat-Affected Zones of Thermite Rail Weldings. Facta Universitatis, Series: Mechanical Engineering, Vol. 22, No. 4, 2024, pp. 689-710, https://doi.org/10.22190/FUME221217008F

[15] B. Magill, Derailments May Increase as 'Sun Kinks' Buckle Tracks, Climate Central, July 31, 2014, Accessed July 30, 2024, https://www.climatecentral.org/news/climate-change-warp-railroad-tracks-sun-kinks-17470

[16] L. Chapman, J. E. Thornes, Y. Huang, X. Cai, V. L. Sanderson, S. P. White, Modelling of Rail Surface Temperatures: A Preliminary Study, Theoretical and Applied Climatology, Vol. 92, No. 1, 2007, pp. 121-131, https://doi.org/10.1007/s00704-007-0313-5

[17] G. B. Kjell, Estimating the Total Risk for a Sun-kink by Measuring Wave Propagation in the Track, Journal of Rail and Rapid Transit, 2014, Vol. 230, https://doi.org/10.1177/0954409714562491

[18] T. C. Millî Eğitim Bakanliği, UKR (Uzun Kaynaklı Ray) 2013, Accessed July 30, 2024, http://www.megep.meb.gov.tr/mte_program_modul/moduller_pdf/UKR%20(Uzun%20Kaynakl%C4%B1%20Ray).pdf

[19] Y. Wu, M. G. Rasul, J. Powell, P. Micenko, M. M. Khan, Rail Temperature Prediction Model, CORE 2012: Global Perspectives, Conference on Railway Engineering, 10-12 September 2012, Brisbane, Australia

[20] C. Esveld, Modern Railway Track, MRT-Productions, Zaltbommel, 2014

[21] G. A. Hunt, An Analysis of Track Buckling Risk, Tech. Rep.: RRTM013, British Railways, 1994

[22] Y. Wu, P. Munro, M. G. Rasul, M. Masud, K. A. Khan, Review on Recent Developments in Rail Temperature Prediction for Use in Buckling Studies, CORE 2010, Rail - Rejuvenation and Renaissance, Conference on Railway Engineering, 12-15 September, 2010, Wellington, New Zealand

[23] Y. Zhang, L. Al-Nazer, G. Carr, Rail Temperature Prediction Model Based on Heat Transfer Principles, Technical Report, Federal Railroad Administration, Washington, DC, USA, Accessed July 30, 2024, https://railknowledgebank.com/Presto/content/GetDoc.axd?ctID=MTk4MTRjNDUtNWQ0My00OTBmLTllYWUtZWFjM2U2OTE0ZDY3&rID=NDIyMQ==&pID=Nzkx&attchmnt=True&uSesDM=False&rIdx=MzIxMw==&rCFU=

[24] Amtrak Engineering, Weather & Rail Temperature Monitoring, Accessed July 30, 2024, https://railtemp.amtrak.com/index.jsp

[25] E. Ferranti, L. Chapman, S. Lee, D. Jaroszweski, C. Lowe, S. Mcculloch, A. Quinn, The Hottest July Day on the Railway Network: Insights and Thoughts for the Future, Meteorological Applications, Vol. 25, No. 2, 2017, pp. 195-208, https://doi.org/10.1002/met.1681

[26] K. Kim, E. Y. Yamashita, Using a K-means Clustering Algorithm to Examine Patterns of Pedestrian Involved Crashes in Honolulu, Hawaii, Journal of Advanced Transportation, Vol. 41, No. 1, 2007, pp. 69-89, http://dx.doi.org/10.1002/atr.5670410106

[27] S. Hong, C. Park, S. Cho, A Rail-Temperature-Prediction Model Based on Machine Learning: Warning of Train-Speed Restrictions Using Weather Forecasting, Sensors, Vol. 21, 2021, https://doi.org/10.3390/s21134606

[28] M. Dick, P. E. R. Bruzek, Comparison of Predicted and Actual Rail Temperature, WRI 2016: 22nd Annual Wheel Rail Interaction Conference, May 2-6, 2016, Henderson, N. V., USA, https://archive.wheel-rail-seminars.com/archives/2016/hh-papers/HH%2013%20Matt%20Dick%202016%20WRI%20Heavy%20Haul.pdf

[29] L. Al-Nazer, Development of a Rail Temperature Prediction Model Based on Heat Transfer Principles, Technical Report, Federal Railroad Administration, Office of Research and Development, Washington, DC, USA, 2012, Accessed July 30, 2024,

https://railroads.dot.gov/sites/fra.dot.gov/files/fra_net/437/RD_Review2012_LAlNazer_RailTemperaturePrediction_FINAL.pdf

[30] Google Earth, Accessed July 30, 2024, https://earth.google.com/web/search/41.57851,+-71.49252/@40.85857801,-79.19773129,601.05441795a,1252425.04758518d,33.90702626y,1.73373361h,33.41729354t,0r/data=CigiJgokCQ4_1c_k4kRAEbH2hu1e4kRAGdES0TCKK1LAITDzKx_tK1LAMikKJwolCiExcDFQaU4ybG1PREFhaHc5Vm9GcUI5VFJjd1FRUTNTUzUgAToDCgEw

[31] Greater Greater Washington, Summer Heat Means Longer Commutes for Trains, Accessed July 30, 2024, https://ggwash.org/view/34153/summer-heat-means-longer-commutes-for-trains

[32] Girardi, L., Boulanger, D., Laurans, E., Pouligny, P., Xu, Y., and Colibri, J.: Rail Temperature Forecasts over Different Time-ranges for Track Applications. in RCM 2011: 5th IET Conference on Railway Condition Monitoring and Non-Destructive Testing, Derby, UK. http://dx.doi.org/10.1049/cp.2011.0609